Fatigue damage propagation and creep behavior on sisal/epoxy composites

Mateus da Silva Batista[1]* , Linconl Araujo Teixeira[1] , Alisson de Souza Louly[1] ,
Sayra Oliveira Silva[1] and Sandra Maria da Luz[1]

[1]*Laboratório de Tecnologias em Biomassa, Departamento de Engenharia Mecânica, Universidade de Brasília – UnB, Brasília, DF, Brasil*

*mateus.s.b@hotmail.com

Abstract

The lack of knowledge about the behavior under creep and fatigue limits the use of polymeric composites reinforced with natural fibers. Thus, this work assessed the behavior of epoxy composites reinforced with sisal fibers under tensile, fatigue, and creep tests. Also, thermogravimetry and scanning electron microscopy assessed the sodium hydroxide (NaOH) treatment efficiency in sisal fibers. Further, differential scanning calorimetry determined the degree of cure of the composites, and stereomicroscopy allowed the evaluation of the surface's fracture. As a result, the tensile strength of the composite was 1.4 times the value of neat epoxy resin after 100,000 cycles in the fatigue test. Moreover, when loaded with 20% of the maximum tensile strength, it is estimated that the composite resists 200,000 h without rupturing by creep. To conclude, the efficient adhesion between sisal fibers and epoxy obtained by NaOH treatment allowed good mechanical behavior to the epoxy composite.

Keywords: *natural fibers, NaOH treatment, mechanical properties, thermal behavior.*

1. Introduction

Although polymer matrix composites reinforced with carbon, glass, or Kevlar fibers have excellent mechanical properties associated with low weight, the use of these synthetic fibers has adverse effects on the environment since their production requires a large amount of energy[1]. Polymeric composites reinforced with natural fibers from plants are attractive alternatives.

There is a wide variety of plants used as reinforcement in polymeric matrices, for example, sisal, jute, palm, curauá, and others. The fibers used as reinforcement come from different plants parts such as the trunk, leaf, fruit branches, and stem[2]. And even if the adhesion between natural fibers and polymers is low, it can be improved with chemical treatments, removing fiber amorphous and nonpolar components and impurities that repel polymers[3]. The treatment with sodium hydroxide (NaOH) is simple and widely used. Palm fruit branch fibers show about 180% greater tensile strength when treated with a NaOH solution, reaching about 290 MPa[2]. In epoxy composites, natural curauá fibers treated with NaOH improve tensile, flexural, and impact strength by 24%, 44%, and 47%, respectively, comparing untreated samples[4]. This sums up the potential of natural fibers for composite applications.

Recently, several studies have reported the mechanical performance of polymeric composites reinforced with natural fibers, but almost all reports use only tensile, flexural, and impact tests. However, more detailed studies on the behavior of polymeric composites reinforced with natural fibers under cyclic loads or quasi-static loads are still required for structural applications. Since composites reinforced with natural fibers are applied for non-structural purposes, such as panels, engine covers, and internal parts of cars and aircraft[5].

Fatigue is the leading cause of failure for failures in aircraft components[6], vehicle storage tanks[7], machine and rail bearings[8], among other engineering applications subjected to cyclic loads. Furthermore, the variability in fatigue properties of the same type of composite due to differences in composition and structure properties requires an understanding of the fatigue mechanism in these materials[9]. Experimental studies are still needed to understand damage propagation and failure modes in composites, and in this sense, the analysis of material stiffness during fatigue tests is used[10]. However, the material's stiffness, which should be reduced with increasing damage to the composites, increases in some cases[11]. Therefore, fatigue tests controlled by strain instead of stress have a consistent behavior with the stiffness of composites, which is reduced until the material breaks[12].

Furthermore, the study of the creep behavior of polymeric composites is also crucial for safe structural design because it presents a time-dependent degradation in stiffness due to strains which can lead to material breakage[13]. The effects

of creep are long-term, and research aims to predict the strength of polymer composites through accelerated testing. However, in general, the tests use temperature variation to accelerate the creep effect on the material, which makes it challenging to obtain results[14]. Therefore, the stepped isostress method (SSM) is a form of life prediction in which the temperature is constant, and what varies is the stress, which is systematically applied to the material[15]. SSM effectively tests amorphous or crystalline polymers and reduces test time by 70 times to predict material life[16].

Although there are reports of epoxy composites reinforced with synthetic fibers under fatigue and creep, few works have studied the performance of composites reinforced with natural fibers. However, natural fibers are promising as reinforcement. For example, hybrid composites of epoxy resin reinforced with fiberglass and kenaf (natural fibers) have fatigue life close to that of material reinforced with only fiberglass[17]. For creep, the stepped isostress method has not yet been reported for composites reinforced with natural fibers. Still, it is promising in predicting the life of polymer composites reinforced with fibers[18].

Therefore, this innovative work intends to promote natural fibers, especially sisal fibers, and provide valuable and new information about the mechanical performance of sisal fibers/epoxy composites under tension-tension fatigue controlled by strain and creep loading tests using the stepped isostress method.

2. Materials and Methods

2.1 Materials

Sisal fibers were supplied by Sisalsul Industry and Commerce LTD (Bahia, Brazil) and treated using sodium hydroxide (NaOH) 97% pure (Greentec) aqueous solution. The polymer matrix is constituted by epoxy resin AR 260, Di-Glycidyl Ether of Bisphenol A (DGEBA), and hardener agent AH 260, Triethylenetetramine (TETA), both supplied by E-composites Commerce of Composite Materials LTD (Rio de Janeiro, Brazil).

2.2 Prepregs and laminated composites obtaining

A superficial treatment was carried out for the sisal fibers soaking them in a 5% (w/v) sodium hydroxide (NaOH) solution with a ratio of 10:1 (solution: fiber). Then, the mix (fibers and sodium hydroxide solution) was kept at 80°C for 2 h under constant stirring. This condition followed the best result from a recent study developed by Teixeira et al.[19]. After, the fibers were washed with distilled water until pH 7. Finally, the fibers were dried at room temperature (~ 25°C) for 96 h and subsequently in an oven (32 °C) for 24 h[20].

The epoxy prepregs were obtained with 15 wt.% of fibers by the hand lay-up method[21]. This fiber content was chosen based on a previous work, where the authors studied the influence of cure agent, treatment, and fiber content by using statistical analysis[22]. Sisal fibers were placed unidirectionally in a steel mold of 200 x 220 mm. The epoxy system was prepared by mixing the resin and hardener in a ratio of 100:21 (epoxy resin: hardener agent), as recommended by the supplier. Then, the resin was spread

on the fibers with a roller. The prepreg was kept at room temperature until it reached stage B, also known as the gel stage, and then kept under refrigeration at -18°C.

Laminated composites were prepared with three unidirectional prepreg layers. The layers were placed in a hydraulic press under a load of 0.5 tons for 1 h. Then, the material was cured at room temperature for 24 h. The post-cure was carried out in the oven at 60°C for 12 h. A neat epoxy resin plate was prepared for a comparison with the composite materials.

2.3 Thermal characterization

Untreated and NaOH-treated sisal fibers, neat uncured epoxy, untreated, and NaOH-treated sisal 15 wt.%/epoxy prepregs were analyzed in a simultaneous TGA-DSC thermal analyzer (SDT Q600, TA Instruments, USA). The samples weighing 10 ± 1 mg were deposited on an alumina pan. The analysis was from 20 to 600°C with a heating rate of 5°C/min under a nitrogen atmosphere at a 50 mL/min flow rate.

TGA was used to assess the surface treatment effect on sisal fibers, and DSC to calculate the degree of cure in the composites, α, determined by Equation 1:

$$\alpha = 1 - \frac{\Delta H_p}{\Delta H_t} \tag{1}$$

where ΔH_p is the partial enthalpy (integral area of the prepregs cure peaks), and ΔH_t is the total enthalpy of the cure reaction (integral area of the uncured epoxy resin cure peak).

2.4 Microscopic analysis

The surface morphology of the treated and untreated sisal fibers was analyzed by scanning electron microscopy (SEM) (TM-4000Plus, Hitachi, Japan), using 15 kV voltage and 400 × magnification. After the rupture in tensile tests, the fracture region of neat epoxy and NaOH-sisal 15 wt.%/epoxy composite specimens were analyzed under a stereomicroscope (DFC-700T, Leica, Germany). The investigated samples were tested before fatigue tests, and 31.5 x magnification and incident light were used.

2.5 Mechanical characterization

2.5.1 Tension-tension fatigue

Tension-tension fatigue tests were carried out according to the American Society for Testing and Materials Standard (ASTM), ASTM D3479[23]. The test was performed on a universal testing machine (8801, Instron, USA) with 100 kN load cell. The test specimen dimensions were 140 × 25 × 3 mm. Tabs of epoxy reinforced with glass fibers of 40 x 25 mm were attached during the composites manufacturing. The fatigue tests were carried out with a frequency of 5 Hz, strain ratio R = 0.1, and controlled by strain. The cyclic load was applied in a sinusoidal waveform with three maximum strain levels (ε_{max}), 0.14, 0.10, and 0.02%. For each strain level, one NaOH-sisal 15 wt.%/epoxy composite specimen and two neat epoxy specimens were analyzed. The pressure on the grips was 15 bar.

The evolution of the dynamic stiffness of the materials during the fatigue tests, E_f, is calculated by the slope of the

secant that links the lowest and the highest peaks in the stress-strain hysteresis loop of each loading cycle. Then it is normalized by the dynamic stiffness of the first cycle, E. The damage propagation during fatigue tests, D, was calculated by $D = 1 - (E_f/E)$[24], where E_f and E are the same mentioned in dynamic stiffness. Dynamic stiffness values and accumulated damage were plotted as a function of loading cycles. The x-axis, N/Nf, presented the number of cycles, N, divided by the maximum number of loading cycles applied to the materials, Nf.

2.5.2 Tensile tests

Tensile tests were performed according to ASTM D3039[25], in two different steps: 1) Tensile before fatigue tests: To measure the maximum tensile strength and determine the maximum stress levels used in creep tests. Five specimens of NaOH-sisal 15 wt.%/epoxy composites specimens (200 × 20 × 3 mm) were tested before fatigue tests using a test machine (Electropuls E10000, Instron, USA) equipped with 10 kN load cell at a speed 2 mm/min. 2) Tensile after fatigue tests: To determine the remaining tensile strength and properties on epoxy composites reinforced with sisal fibers and neat epoxy samples that reached the run-out on fatigue tests, defined as 100,000 cycles. For each strain level in fatigue tests, one NaOH-sisal 15 wt.%/epoxy composite specimen and two neat epoxy specimens were tested. The specimen size was 140 × 25 × 3 mm, manufactured with tabs, and the tests were performed using a test machine (8801, Instron, USA) equipped with a 100 kN load cell at a speed of 0.3 mm/min. In these tests, the presence of tabs influenced the premature rupture of the material, so the execution speed was lower than that of the previous tensile test, used to determine the stress levels of the creep test.

2.5.3 Creep

Creep tests were performed using a test machine (ElectroPuls E10000, Instron, USA) equipped with a 10 kN load cell and mechanical grips. The NaOH-sisal 15 wt.%/epoxy composite rectangular specimens (200 × 20 × 3 mm) were manufactured without tabs and tested before fatigue tests. The creep test was performed according to the Stepped Isostress Method (SSM)[15]. Different loads are applied to a specimen during the same test at 25oC. The loads were changed at a staggering rate: 20% (12.98 MPa), 25% (16.23 MPa), 30% (19.46 MPa), 35% (22.72 MPa), and 40% (19.48 MPa) of the ultimate tensile strength of the specimen. After the first stress level was defined, the tension was maintained on the material for 3 h for each tension step. With these measurements, the strain vs time curve was made.

From the curve from the experimental data of strain vs time, three shifts in the curve were made: the vertical, rescaling, and horizontal. For the vertical shift, each step of the initial curve is adjusted by Equation 2:

$$\varepsilon = Ci * \left(t - t_{0i} \right) n \tag{2}$$

where ε is the strain, t is the time, Ci and n are materials constants, t_{0i} is the point where the i-th fitting curve crosses the abscissa. Second, the rescaling shift, each step of the curve is discounted by t_{0i}. This shifts each step to the left. Finally, in horizontal shift, the curve points are divided by a displacement factor, as obtained by Equation 3:

$$a_s = \left(\frac{C_0}{C_i} \right)^{\frac{1}{n}} \tag{3}$$

where C_0 is the coefficient C_I of the first level of strain. The creep curves are plotted with these strains vs the log time, estimating the strain after long periods.

3. Results and Discussion

3.1 Effect of chemical treatment on sisal fibers' morphology

The structural morphology of sisal fibers for untreated and NaOH-treated sisal fibers can be seen in SEM images in Figure 1. The chemical treatment removed part of the hemicellulose layers on the surface of sisal fibers, presented in Figure 1a, facilitating the adhesion between the fibers and the polymeric matrix. Thus, bundles of cellulose fibrils, a component with a high percentage of crystallinity and mechanical resistance, are exposed, as shown in Figure 1b. The adhesion between the reinforcement and the polymeric matrix could improve due to the significant surface roughness of fibers and the effective contact area[26,27]. In previous work, the treatment conditions applied to natural fibers
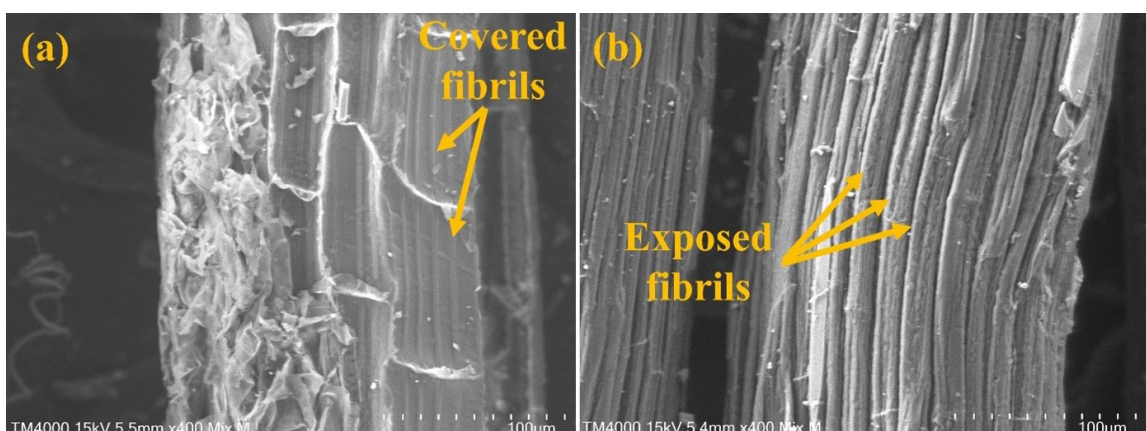
Figure 1. Scanning electron microscopy (SEM) for untreated (a) and NaOH-treated sisal fibers (b).

(5% solution, for 2 h at 80°C) improved its crystallinity. Also, the hemicellulose was removed without losses in cellulose content[19].

3.2 Thermal characterization

Figures 2a and b show the TG and DTG curves for samples of untreated and NaOH-treated sisal fibers, respectively. The degradation steps are indicated in the TG curves. The first step, from 30-105 °C for untreated and 30-150 °C for treated fibers, is associated with loss of moisture absorbed by the fibers (about 5% weight loss). In treated fibers, the range of temperature is higher, as the treatment increases its moisture absorption[28]. In the second step, the degradation of fiber components begins at 160°C for the untreated fiber and refers to the degradation of hemicellulose

(about 20% weight loss) followed by cellulose degradation (about 40% loss weight) in the third step.

The untreated fibers showed two degradation peaks at 280 °C and 340 °C (DTG curves), corresponding to hemicellulose and cellulose degradation, respectively[29]. The treated fibers, however, have a single cellulose degradation stage (about 60% weight loss), which starts at 230 °C, indicating an increase in the thermal stability of the fibers by 50 °C. The increase in the thermal stability of the fibers happens because the alkali treatment with NaOH removes hemicellulose, which has low thermal stability[30].

In previous work, the components losses are followed by chemical characterization and Fourier transform infrared spectroscopy, confirming the effects of the treatments on hemicellulose and cellulose thermal degradation. The degradation steps (TG curves), for untreated (fourth step) and treated
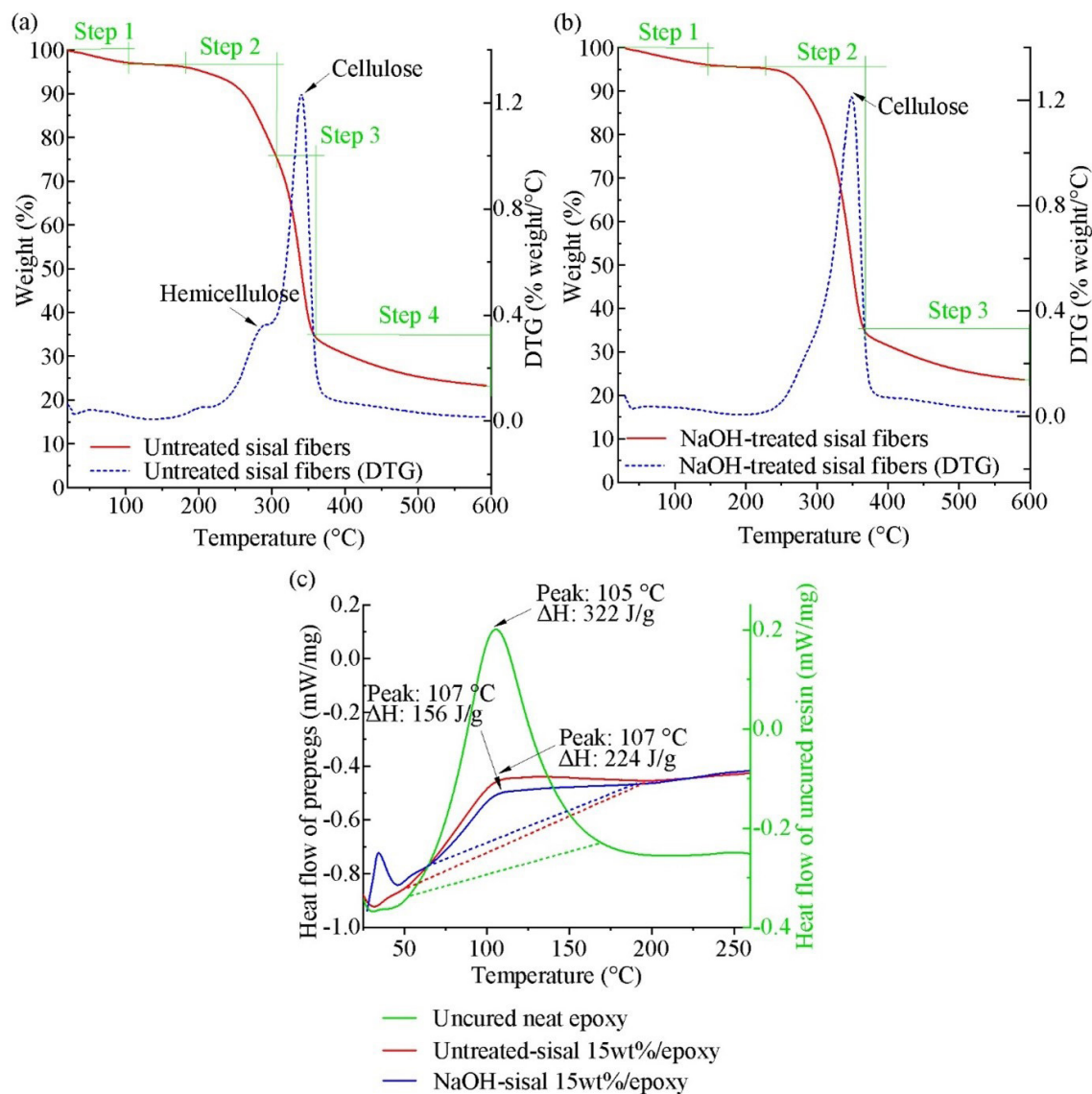
Figure 2. TG and DTG curves for untreated sisal fibers (a) and NaOH-treated sisal fibers (b); DSC curves for neat uncured epoxy, untreated-sisal 15 wt.%/epoxy, and NaOH-sisal 15 wt.%/epoxy (c).

fibers (third step) are linked to lignin degradation (about 12% weight loss)[29]. A residue of 23% in weight of the carbonized fibers was observed. In our previous work with the same epoxy and fiber content, 15 wt.%, also presented high thermal stability[31].

Through the DSC analyzes, it is possible to observe the exothermic peaks of the prepregs. Figure 2c shows the DSC curves for sisal (NaOH treated and untreated) 15 wt.%/epoxy prepregs compared to uncured neat epoxy resin. The first exothermic peak, around 40 °C, is related to the glass transition temperature of epoxy and agrees with what is reported in the literature[32]. The exothermic peaks around 100°C are related to the curing reactions of the crosslinks in the epoxy resin[21]. Enthalpy is the energy released by the system in the formation of crosslinks, calculated by the area under the peak curing temperature in DSC curves delimited by the baselines (dashed lines). The degree of cure of prepregs is inverse to the enthalpy value. The higher degree of cure is related to the more significant crosslinking number in the epoxy resin matrix and the elevated mechanical resistance of the composite[33]. The high crosslink content in epoxy resins reduces the strain rate of the material, increases its recovery capacity, and affects the fatigue strength of epoxy resin-based materials[34].

The degree of cure of NaOH-sisal/epoxy prepreg was 51.55%, 1.7 times higher than that of untreated sisal/epoxy prepregs (30.36%). The presence of hydroxyl groups, OH, increases the number of cross-links established between the resin and the curing agent[35]. The chemical treatment exposes the cellulose chains of the natural fibers and their OH groups, hence the higher concentration of cross-links in the treated sisal-reinforced prepreg. In addition, the treatment on sisal fibers allows a higher crosslinked interphase due to the intermediate module between reinforcement and polymer[36]. Undoubtedly, it influenced the better fatigue and tensile strength for NaOH-sisal 15 wt.%/epoxy composites compared to neat epoxy, as discussed in the following section.

3.3 Laminated composites characterization

Figures 3a and 3b shows the stiffness loss of neat epoxy and NaOH-sisal 15 wt.%/epoxy composite during the fatigue tests, respectively. For all materials, a dynamic stiffness loss during the fatigue tests is observed. This behavior is as expected, presenting the stiffness reduction[37]. When comparing the materials, at 0.14% of maximum strain, the stiffness loss was lower, about 3% for the composite. However, the composite was more resistant to fatigue than neat epoxy because the fibers transfer the applied load and provide a barrier preventing crack propagation in composites[38]. The stiffness is reduced because only part of the energy released in the loading is recovered[39].
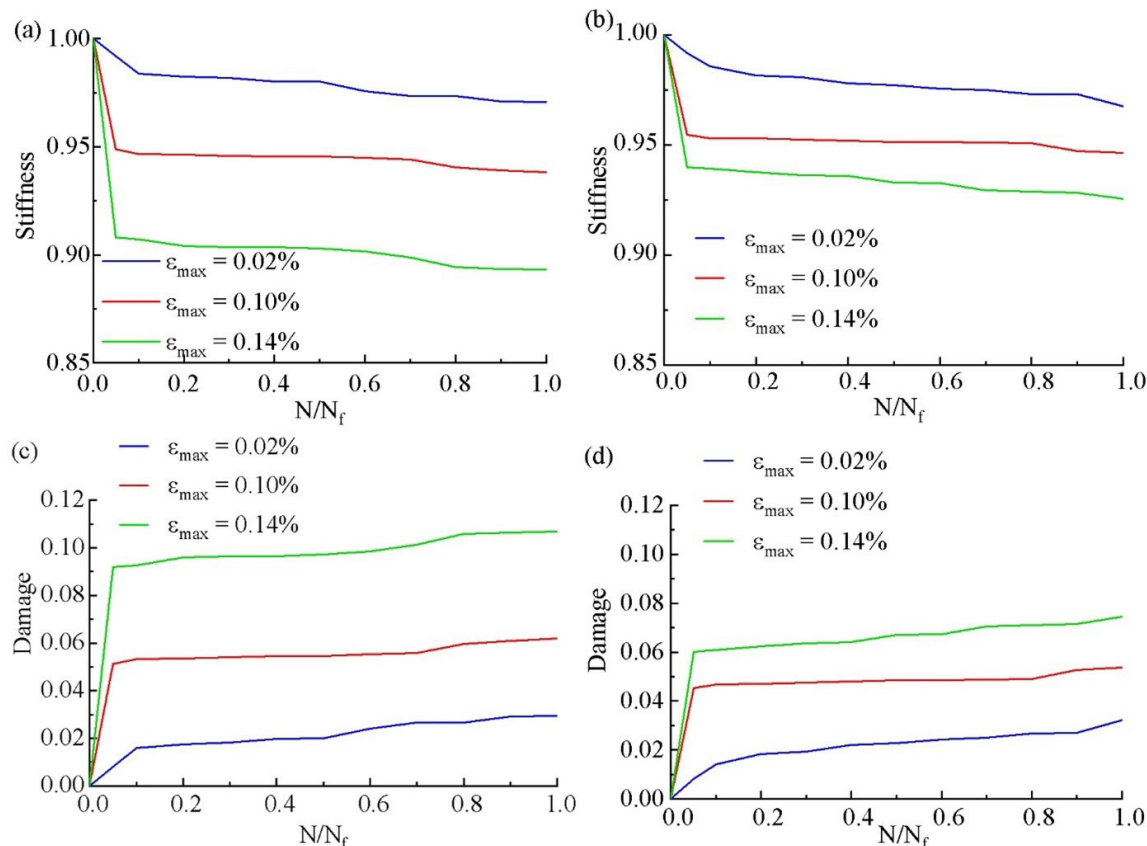
Figure 3. Normalized dynamic stiffness during fatigue tests for (a) neat epoxy; and (b) NaOH-sisal 15 wt.%/epoxy; and damage propagation during fatigue tests for (c) neat epoxy; and (d) NaOH-sisal 15 wt.%/epoxy.

Figures 3c and 3d show the accumulated damage during fatigue tests of neat epoxy and NaOH-sisal 15 wt.%/epoxy composite, respectively. The presented damage curve is expected because damage to epoxy composites is inversely proportional to degradation in stiffness[40]. This is also reflected in a consistent damage curve representation. Strain control prevents the false increase in dynamic stiffness by residual strains observed for some epoxy composites reinforced with natural fibers in fatigue tests[12].

After the run-out in fatigue tests, the specimens were tested under tensile. The properties of neat epoxy and NaOH-sisal 15 wt.%/epoxy composite are shown in Table 1, where ε_{max} is the maximum strain applied during fatigue tests cycles. The addition of treated sisal fibers to the epoxy resin increased the tensile strength by about 40%, achieving 47 MPa against 34 MPa of neat epoxy. The found values are as expected for tensile strength of epoxy composites reinforced with aligned sisal fibers, 51.5 ± 5.6 MPa[41], and superior to epoxy composites reinforced with jute fabrics, 40 MPa of tensile strength[42]. In general, composites reinforced with unidirectional fibers have better tensile properties than those reinforced with woven fabrics due to the undulations in the yarn which form the fabric structure[43]. In addition, the NaOH-sisal 15 wt.%/epoxy composite presented superior tensile strength comparing epoxy composites reinforced with 10 wt.% of untreated sisal fibers, by 50%[44].

In addition, the tested specimens broke at the base of tabs. Silva et al.[21], reported a 40% higher tensile strength for NaOH-treated sisal fibers (15 wt.%) epoxy composites in samples manufactured without tabs and not subjected to cycles, showing the negative influence of these conditions on the tensile properties of the material. The presence of tabs can cause the premature rupture of the specimens due to the increase in the concentration of stresses caused by geometric discontinuities among the parts[45].

The stress level used in creep tests was also determined by testing NaOH-sisal 15 wt.%/epoxy under tensile. The samples presented 64.86 ± 12.20 MPa on tensile strength and 5.04 ± 0.49 GPa on Young's Modulus, as shown in Table 1. This tensile strength is similar to the value given for epoxy composites reinforced with glass fibers[46].

Stereomicroscopy was used to analyze the morphology of surface fracture of the neat epoxy and NaOH-sisal 15 wt.%/epoxy composites materials after the tensile tests, as shown in Figure 4. The specimens were manufactured without tabs and tested before fatigue tests. The micrograph of neat epoxy resin, Figure 4a, shows the cracks propagation without material flow and the absence of voids and defects in the epoxy resin. This region is flat, not reflective, has riverbed patterns, and demonstrates its brittle characteristics[47]. The river lines with a smooth surface are due to the excellent bonding of the epoxy resin[48].

Figure 4b shows the NaOH-sisal 15 wt.%/epoxy composite, and it is possible to observe the fiber rupture. Compared with neat epoxy resin, the best mechanical performance is linked to the efficient adhesion between sisal fiber and epoxy

Table 1. Tensile properties for neat epoxy and NaOH-sisal 15 wt%/epoxy composite specimens.

Sample	ε_{max} (%)	UTS (MPa)	Max. Elongation (%)	Young's Modulus (GPa)
NaOH-sisal 15 wt.%/epoxy*	-	64.9 ± 12.2	1.7 ± 0.4	5.0 ± 0.5
Neat epoxy	0.02	31.8 ± 2.3	1.1 ± 0.1	2.9 ± 0.1
Neat epoxy	0.10	35.4 ± 0.6	1.3 ± 0.1	2.8 ± 0.2
Neat epoxy	0.14	35.1 ± 11.9	1.3 ± 0.5	2.7 ± 0.1
NaOH-sisal 15 wt.%/epoxy	0.02	51.0	1.9	3.0
NaOH-sisal 15 wt.%/epoxy	0.10	48.9	1.9	3.1
NaOH-sisal 15 wt.%/epoxy	0.14	46.2	1.8	3.1

* NaOH-sisal/epoxy specimens manufactured without tabs and tested before the fatigue tests.
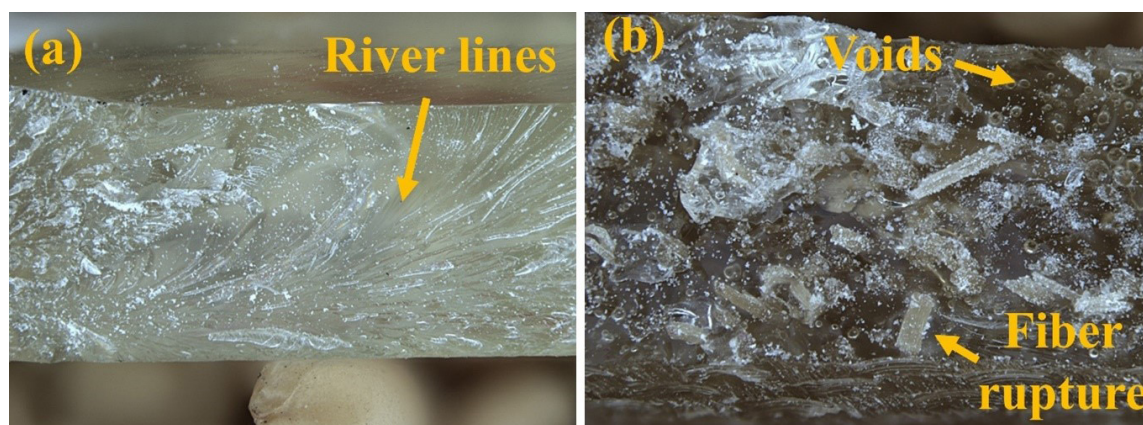
Figure 4. Stereomicroscopy of a fractured surface of the specimens after the tensile tests for (a) neat epoxy; and (b) NaOH-sisal 15 wt.%/epoxy.
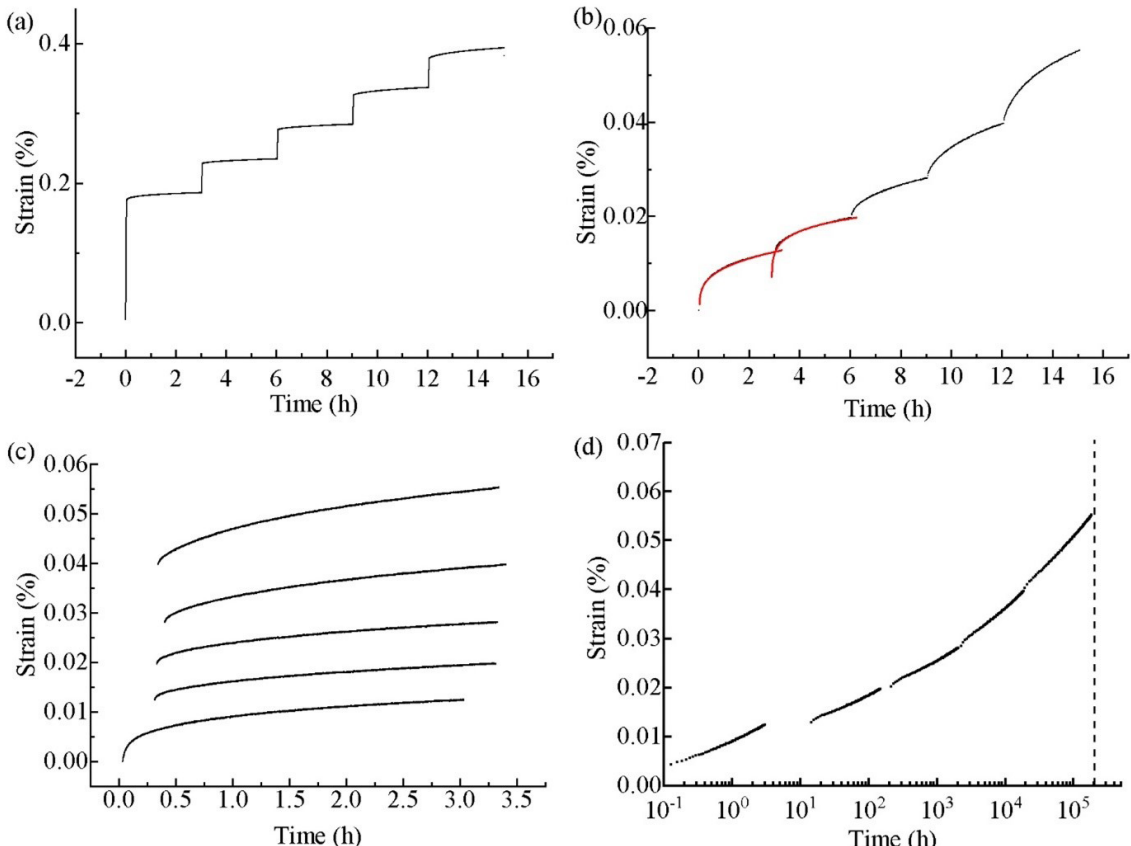
Figure 5. Creep results for (a) Strain vs time curve for NaOH-sisal 15 wt.%/epoxy composite; Vertical shift (b), and rescaling shift for NaOH-sisal 15 wt.%/epoxy composite (c); and Stepped Isostress Method (SSM) curve for NaOH-sisal 15 wt.%/epoxy composite (d).

resin. In addition, voids are observed, defects caused by the release of volatiles and trapping of the gases generated in the resin curing reactions during the manufacturing process. The presence of voids in the epoxy resin reduces its tensile properties, but resin degassing with an ultrasonic bath, as was done in this work, improves its tensile strength[49]. Also, in recent literature, alkali-pretreatment jute fibers (natural fibers) reduce the number of epoxy composites voids and increase their tensile strength[50].

Figure 5a shows the strain vs time curve obtained for NaOH-sisal/epoxy composites after the creep test. It is possible to observe that strain increases with each step's time (20, 25, 30, 35, and 40% of UTS). Figures 5b and 5c show the vertical and rescaling shifts, respectively. Finally, Figure 5d shows the Stepped Isostress Method (SSM) curve and, according to this, it is valid to state that with 20% UTS the material resists for 200,000 hours without undergoing a creep break. This is due to the insertion of natural fibers in the composite, as the incorporation of fibers can successfully reduce creep since the tension transmitted to the matrix can be transferred to the fibers before the material breaks[51].

4. Conclusions

In conclusion, the NaOH treatment removed hemicellulose and increased its thermal stability. Also, the NaOH-sisal

15wt.%/epoxy composites present the best strength under fatigue and tensile compared to neat epoxy. This behavior can be explained by adding unidirectional sisal fibers with high tensile strength when the load is applied on its longitudinal axis. Due to the NaOH treatment of the sisal fibers, the adhesion between the fiber and the epoxy matrix was also efficient in distributing loads applied to the composite. The more significant crosslinks number was observed for the NaOH-sisal 15 wt.%/epoxy compared to the neat epoxy. The higher crosslink content also contributed to the higher fatigue and tensile strength of the material. These characteristics were also significant in the resistance of the composite against creep.

5. Acknowledgements

6. References

1. Fitzgerald, A., Proud, W., Kandemir, A., Murphy, R. J., Jesson, D. A., Trask, R. S., Hamerton, I., & Longana, M. L. (2021).

A life cycle engineering perspective on biocomposites as a solution for a sustainable recovery. *Sustainability*, *13*(3), 1160. http://dx.doi.org/10.3390/su13031160.

2. Amroune, S., Bezazi, A., Dufresne, A., Scarpa, F., & Imad, A. (2021). Investigation of the date palm fiber for green composites reinforcement: thermo-physical and mechanical properties of the fiber. *Journal of Natural Fibers*, *18*(5), 717-734. http://dx.doi.org/10.1080/15440478.2019.1645791.

3. Bezazi, A., Boumediri, H., Garcia del Pino, G., Bezzazi, B., Scarpa, F., Reis, P. N. B., & Dufresne, A. (2020). Alkali treatment effect on physicochemical and tensile properties of date palm rachis fibers. *Journal of Natural Fibers*, 1-18. http://dx.doi.org/10.1080/15440478.2020.1848726.

4. del Pino, G. G., Bezazi, A., Boumediri, H., Kieling, A. C., Silva, C. C., Dehaini, J., Rivera, J. L. V., Valenzuela, M. G. S., Díaz, F. R. V., & Panzera, T. H. (2021). Hybrid epoxy composites made from treated curauá fibres and organophilic clay. *Journal of Composite Materials*, *55*(1), 57-69. http://dx.doi.org/10.1177/0021998320945785.

5. Muthu, S. S. (Ed.) (2019). Green composites. Singapore: Springer. http://dx.doi.org/10.1007/978-981-13-1972-3.

6. Tavares, S. M. O., & Castro, P. M. S. T. (2017). An overview of fatigue in aircraft structures. *Fatigue & Fracture of Engineering Materials & Structures*, *40*(10), 1510-1529. http://dx.doi.org/10.1111/ffe.12631.

7. Zhang, M., Lv, H., Kang, H., Zhou, W., & Zhang, C. (2019). A literature review of failure prediction and analysis methods for composite high-pressure hydrogen storage tanks. *International Journal of Hydrogen Energy*, *44*(47), 25777-25799. http://dx.doi.org/10.1016/j.ijhydene.2019.08.001.

8. Guo, W., Cao, H. R., Zi, Y. Y., & He, Z. J. (2018). Material analysis of the fatigue mechanism of rollers in tapered roller bearings. *Science China. Technological Sciences*, *61*(7), 1003-1011. http://dx.doi.org/10.1007/s11431-017-9249-2.

9. Hamidi, H., Xiong, W., Hoa, S. V., & Ganesan, R. (2018). Fatigue behavior of thick composite laminates under flexural loading. *Composite Structures*, *200*, 277-289. http://dx.doi.org/10.1016/j.compstruct.2018.05.149.

10. Vassilopoulos, A. P. (2020). The history of fiber-reinforced polymer composite laminate fatigue. *International Journal of Fatigue*, *134*, 105512. http://dx.doi.org/10.1016/j.ijfatigue.2020.105512.

11. Liang, S., Gning, P. B., & Guillaumat, L. (2012). A comparative study of fatigue behaviour of flax/epoxy and glass/epoxy composites. *Composites Science and Technology*, *72*(5), 535-543. http://dx.doi.org/10.1016/j.compscitech.2012.01.011.

12. Mahboob, Z., & Bougherara, H. (2020). Strain amplitude controlled fatigue of Flax-epoxy laminates. *Composites. Part B, Engineering*, *186*, 107769. http://dx.doi.org/10.1016/j.compositesb.2020.107769.

13. Jia, Y., & Fiedler, B. (2020). Tensile creep behaviour of unidirectional flax fibre reinforced bio-based epoxy composites. *Composites Communications*, *18*, 5-12. http://dx.doi.org/10.1016/j.coco.2019.12.010.

14. Achereiner, F., Engelsing, K., Bastian, M., & Heidemeyer, P. (2013). Accelerated creep testing of polymers using the stepped isothermal method. *Polymer Testing*, *32*(3), 447-454. http://dx.doi.org/10.1016/j.polymertesting.2013.01.014.

15. Guedes, R. M. (2018). A systematic methodology for creep master curve construction using the stepped isostress method (SSM): a numerical assessment. *Mechanics of Time-Dependent Materials*, *22*(1), 79-93. http://dx.doi.org/10.1007/s11043-017-9353-0.

16. Fairhurst, A., Thommen, M., & Rytka, C. (2019). Comparison of short and long term creep testing in high performance polymers. *Polymer Testing*, *78*, 105979. http://dx.doi.org/10.1016/j.polymertesting.2019.105979.

17. Feng, N. L., Dharmalingam, S., Zakaria, K. A., & Selamat, M. Z. (2019). Investigation on the fatigue life characteristic of kenaf / glass woven-ply reinforced metal sandwich materials. *The Journal of Sandwich Structures & Materials*, *21*(7), 2440-2455. http://dx.doi.org/10.1177/1099636217729910.

18. Tanks, J., Rader, K., Sharp, S., & Sakai, T. (2017). Accelerated creep and creep-rupture testing of transverse unidirectional carbon/epoxy lamina based on the stepped isostress method. *Composite Structures*, *159*, 455-462. http://dx.doi.org/10.1016/j.compstruct.2016.09.096.

19. Teixeira, L. A., Dalla, L. V., Jr., & Luz, S. M. (2021). Chemical treatment of curaua fibres and its effect on the mechanical performance of fibre/polyester composites. *Plastics, Rubber and Composites*, *50*(4), 189-199. http://dx.doi.org/10.1080/14658011.2020.1862978.

20. Spinacé, M. A. S., Lambert, C. S., Fermoselli, K. K. G., & De Paoli, M.-A. (2009). Characterization of lignocellulosic curaua fibres. *Carbohydrate Polymers*, *77*(1), 47-53. http://dx.doi.org/10.1016/j.carbpol.2008.12.005.

21. Silva, S. O., Teixeira, L. A., Gontijo, A. B., & Luz, S. M. (2021). Processing Characterization of Sisal/Epoxy Prepregs. *Journal of Research Updates in Polymer Science*, *10*, 42-50. http://dx.doi.org/10.6000/1929-5995.2021.10.6.

22. Libera, V. D., Jr., Leão, R. M., Steier, V. F., & Luz, S. M. (2020). Influence of cure agent, treatment and fibre content on the thermal behaviour of a curaua/epoxy prepreg. *Plastics, Rubber and Composites*, *49*(5), 214-221. http://dx.doi.org/10.1080/14658011.2020.1729658.

23. American Society for Testing and Materials – ASTM. (2012). ASTM D3479/D3479M-12: Standard Test Method for Tension-Tension Fatigue of Polymer Matrix Composite Materials. West Conshohocken: ASTM. http://dx.doi.org/10.1520/D3479_D3479M-12.

24. Venkatachalam, S., & Murthy, H. (2018). Damage characterization and fatigue modeling of CFRP subjected to cyclic loading. *Composite Structures*, *202*, 1069-1077. http://dx.doi.org/10.1016/j.compstruct.2018.05.030.

25. American Society for Testing and Materials – ASTM. (2017). ASTM D3039/D3039M-17: Standard Test Method for Tensile Properties of Polymer Matrix Composite Materials. West Conshohocken: ASTM. http://dx.doi.org/10.1520/D3039_D3039M-17.

26. Sreekumar, P. A., Thomas, S. P., Saiter, J., Joseph, K., Unnikrishnan, G., & Thomas, S. (2009). Effect of fiber surface modification on the mechanical and water absorption characteristics of sisal/polyester composites fabricated by resin transfer molding. *Composites. Part A, Applied Science and Manufacturing*, *40*(11), 1777-1784. http://dx.doi.org/10.1016/j.compositesa.2009.08.013.

27. Koronis, G., Silva, A., & Fontul, M. (2013). Green composites: a review of adequate materials for automotive applications. *Composites. Part B, Engineering*, *44*(1), 120-127. http://dx.doi.org/10.1016/j.compositesb.2012.07.004.

28. Gudayu, A. D., Steuernagel, L., Meiners, D., & Gideon, R. (2020). Effect of surface treatment on moisture absorption, thermal, and mechanical properties of sisal fiber. *Journal of Industrial Textiles*, 1-21. http://dx.doi.org/10.1177/1528083720924774.

29. Chaitanya, S., & Singh, I. (2018). Sisal fiber-reinforced green composites: effect of ecofriendly fiber treatment. *Polymer Composites*, *39*(12), 4310-4321. http://dx.doi.org/10.1002/pc.24511.

30. Chaishome, J., & Rattanapaskorn, S. (2017). The influence of alkaline treatment on thermal stability of flax fibres. *IOP Conference Series. Materials Science and Engineering*, *191*, 012007. http://dx.doi.org/10.1088/1757-899X/191/1/012007.

31. Libera, V. D., Jr. (2019). *Laminados de fibra de curauá/epóxi obtidos a partir de pré-impregnados* (Dissertação de mestrado). Universidade de Brasília, Brasília. Retrieved in 2021, November 15, from https://repositorio.unb.br/handle/10482/35728

32. Libera, V. D., Teixeira, L. A., Leão, R. M., & Luz, S. M. (2019). Evaluation of thermal behavior and cure kinetics of a curauá fiber prepreg by the non-isothermal method. *Materials Today: Proceedings*, *8*(Pt 3), 839-846. http://dx.doi.org/10.1016/j.matpr.2019.02.026.

33. Vidil, T., Tournilhac, F., Musso, S., Robisson, A., & Leibler, L. (2016). Control of reactions and network structures of epoxy thermosets. *Progress in Polymer Science*, *62*, 126-179. http://dx.doi.org/10.1016/j.progpolymsci.2016.06.003.

34. Hu, X., Wang, Y., Yu, J., Zhu, J., & Hu, Z. (2017). The mechanical and fatigue properties of flowable crosslink thermoplastic polymer blends based on self-catalysis of transesterification. *Journal of Applied Polymer Science*, *134*(24), 1-9. http://dx.doi.org/10.1002/app.44964.

35. Salasinska, K., Barczewski, M., Górny, R., & Kloziński, A. (2018). Evaluation of highly filled epoxy composites modified with walnut shell waste filler. *Polymer Bulletin*, *75*(6), 2511-2528. http://dx.doi.org/10.1007/s00289-017-2163-3.

36. Venkatachalam, N., Navaneethakrishnan, P., Rajsekar, R., & Shankar, S. (2016). Effect of pretreatment methods on properties of natural fiber composites: a review. *Polymers & Polymer Composites*, *24*(7), 555-566. http://dx.doi.org/10.1177/096739111602400715.

37. Van Paepegem, W., & Degrieck, J. (2002). A new coupled approach of residual stiffness and strength for fatigue of fibre-reinforced composites. *International Journal of Fatigue*, *24*(7), 747-762. http://dx.doi.org/10.1016/S0142-1123(01)00194-3.

38. Chawla, K. K. (2019). *Designing with composites.* In: K. K. Chawla (Ed.), *Composite materials* (pp. 491-501). USA: Springer International Publishing.

39. Bensadoun, F., Vallons, K. A. M., Lessard, L. B., Verpoest, I., & Van Vuure, A. W. (2016). Fatigue behaviour assessment of flax–epoxy composites. *Composites. Part A, Applied Science and Manufacturing*, *82*, 253-266. http://dx.doi.org/10.1016/j.compositesa.2015.11.003.

40. Padmaraj, N. H., Vijaya, K. M., & Dayananda, P. (2020). Experimental study on the tension-tension fatigue behaviour of glass/epoxy quasi-isotropic composites. *Journal of King Saud University - Engineering Science*, *32*(6), 396-401. http://dx.doi.org/10.1016/j.jksues.2019.04.007.

41. Webo, W., Maringa, M., & Masu, L. (2020). The combined effect of mercerisation, silane treatment and acid hydrolysis on the mechanical properties of sisal fibre/epoxy resin composites. *MRS Advances*, *5*(23), 1225-1233. http://dx.doi.org/10.1557/adv.2020.122.

42. Cavalcanti, D. K. K., Banea, M. D., Neto, J. S. S., Lima, R. A. A., Silva, L. F. M., & Carbas, R. J. C. (2019). Mechanical characterization of intralaminar natural fibre-reinforced hybrid composites. *Composites. Part B, Engineering*, *175*, 107149. http://dx.doi.org/10.1016/j.compositesb.2019.107149.

43. Mallick, P. K. (2007). Fiber-reinforced composites materials, manufacturing, and design. USA: CRC Press. http://dx.doi.org/10.1201/9781420005981.

44. Yadav, D., Selokar, G. R., Agrawal, A., Mishra, V., & Khan, I. A. (2021). Effect of concentration of NaOH treatment on mechanical properties of epoxy/sisal fiber composites. *IOP Conference Series. Materials Science and Engineering*, *1017*(1), 012028. http://dx.doi.org/10.1088/1757-899X/1017/1/012028.

45. Kobeissi, A., Rahme, P., Leotoing, L., & Guines, D. (2020). Strength characterization of glass/epoxy plain weave composite under different biaxial loading ratios. *Journal of Composite Materials*, *54*(19), 2549-2563. http://dx.doi.org/10.1177/0021998319899135.

46. Queiroz, H. F. M., Banea, M. D., & Cavalcanti, D. K. K. (2020). Experimental analysis of adhesively bonded joints in synthetic- and natural fibre-reinforced polymer composites. *Journal of Composite Materials*, *54*(9), 1245-1255. http://dx.doi.org/10.1177/0021998319876979.

47. Wu, T., Liu, Y., Li, N., Huang, G.-W., Qu, C.-B., & Xiao, H.-M. (2019). Cryogenic mechanical properties of epoxy resin toughened by hydroxyl-terminated polyurethane. *Polymer Testing*, *74*, 45-56. http://dx.doi.org/10.1016/j.polymertesting.2018.11.048.

48. Sathishkumar, G. K., Gautham, G., Shankar, G. G., Rajkumar, G., Karpagam, R., Dhivya, V., Zacharia, G., Gopinath, B., Karthik, P., & Charles, M. M. (2021). Influence of lignite fly ash on the structural and mechanical properties of banana fiber containing epoxy polymer matrix composite. *Polymer Bulletin*, *79*(1), 285-306. http://dx.doi.org/10.1007/s00289-020-03524-6.

49. Oliveira, A., Becker, C. M., & Amico, S. C. (2015). Avaliação das características da resina epóxi com diferentes aditivos desaerantes. *Polímeros*, *25*(2), 186-191. http://dx.doi.org/10.1590/0104-1428.1661.

50. Wang, H., Memon, H., Hassan, E. A. M., Miah, M. S., & Ali, M. A. (2019). Effect of jute fiber modification on mechanical properties of jute fiber composite. *Materials (Basel)*, *12*(8), 1226. http://dx.doi.org/10.3390/ma12081226. PMid:30991643.

51. Wong, S., & Shanks, R. (2008). Creep behaviour of biopolymers and modified flax fibre composites. *Composite Interfaces*, *15*(2-3), 131-145. http://dx.doi.org/10.1163/156855408783810894.